



Providing Choice & Value

Generic CT and MRI Contrast Agents



FRESENIUS
KABI

CONTACT REP

AJNR

Diffusion Anisotropy of the Internal Capsule and the Corona Radiata in Association with Stroke and Tumors as Measured by Diffusion-weighted MR Imaging

Shuichi Higano, Jianhui Zhong, David A. Shrier, Dean K. Shibata, Yukinori Takase, Henry Wang and Yuji Numaguchi

This information is current as of July 25, 2025.

AJNR Am J Neuroradiol 2001, 22 (3) 456-463
<http://www.ajnr.org/content/22/3/456>

Diffusion Anisotropy of the Internal Capsule and the Corona Radiata in Association with Stroke and Tumors as Measured by Diffusion-weighted MR Imaging

Shuichi Higano, Jianhui Zhong, David A. Shrier, Dean K. Shibata, Yukinori Takase, Henry Wang, and Yuji Numaguchi

BACKGROUND AND PURPOSE: Diffusion-weighted MR images have enabled measurement of directionality of diffusion (anisotropy) in white matter. To investigate differences in the anisotropy for various types of pathologic findings and the association between the anisotropy of tracts and neurologic dysfunction, we compared the anisotropy of the posterior limb of the internal capsule and the corona radiata between patients with stroke and those with tumors and between patients with and without hemiparesis.

METHODS: Thirty-three patients consisting of 11 with tumors and 22 with ischemic disease (16 acute infarction, four old infarction, and two transient ischemic attack) and nine control patients were studied with a 1.5-T MR imager. Diffusion-weighted images were obtained with diffusion gradients applied in three orthogonal directions. The diffusion anisotropy measurements were obtained from regions of interests defined within the internal capsule and the corona radiata.

RESULTS: The diffusion anisotropy was significantly reduced in all internal capsules and coronae radiata involved by infarcts, tumors, and peritumoral edema compared with that of the control patients ($P < .0001$). This reduction was most prominent in the tracts involved by tumors ($P < .05$). The anisotropy of the internal capsules and coronae radiata was significantly decreased in cases with moderate-to-severe hemiparesis as compared with those with no or mild hemiparesis ($P < .0001$). Diffusion anisotropy tended to be also reduced in normal-appearing internal capsules and coronae radiata that were remote from the involved segment of the corticospinal tract.

CONCLUSION: The degree of impaired diffusion anisotropy may vary in different pathologic conditions and correlate with neurologic dysfunction. The measurement of diffusion anisotropy may provide additional information relating to neurologic function and transneuronal effects.

Diffusion-weighted imaging is a method of MR imaging that is sensitive to the random motion (diffusion) of water molecules. Using specific pulses (motion-probing gradients), the phase differences between mobile protons and immobile ones are accentuated (1, 2). On diffusion-weighted images, therefore, MR signal decreases in regions

in which water diffusion rates are high and increases in areas that have more restricted diffusion. The magnitude of water diffusion (ie, the apparent diffusion coefficient) is known to change in various pathologic conditions, including ischemic disease, brain tumor, and demyelinating diseases (3–10).

In addition to the pathologic state, the water diffusion is varied in normal brain tissue. In the myelinated white matter, the water molecules move relatively freely in the direction parallel to the fiber tracts but are restricted in their movement perpendicular to the tracts, which is called *diffusion anisotropy* (11–14). Recently, diffusion-weighted images with several different directional motion-probing gradients have enabled evaluation of the magnitude and directionality of water diffusion (15, 16). With this technique, diffusion-weighted imaging has been used for investigation of white matter (eg, visualization of long fiber tracts) and for

Received December 1, 1999; accepted after revision August 8, 2000.

From the Department of Radiology (S.H., J.Z., D.A.S., D.K.S., Y.T., H.W., Y.N.), Division of Neuroradiology, University of Rochester Medical Center, Rochester, NY.

A summary of this work was presented at the 37th Annual Meeting of the American Society of Neuroradiology, San Diego, CA, April 1999.

Address reprint requests to Yuji Numaguchi, MD, PhD, Department of Radiology, Division of Neuroradiology, University of Rochester Medical Center, 601 Elmwood Avenue, Box 648, Rochester, NY 14642.

determining changes in diffusion anisotropy when lesions involve white matter tracts (17–21).

Some studies have shown that diffusion anisotropy in the white matter and the apparent diffusion coefficient change under pathologic conditions (17, 22–26). As far as we know, however, there have been no reports evaluating changes in the anisotropy of white matter tracts in various disease states. Several investigators have examined the relationship between involved and/or dysfunctional tracts and diffusion anisotropy (17, 20, 24). The purposes of this study were to compare diffusion anisotropy in white matter tracts of patients with various types of pathologic findings and to investigate the association between anisotropy of the tracts and neurologic dysfunction. We chose supratentorial segments of the corticospinal tract (the posterior limb of the internal capsule and the corona radiata) as a target for investigation, and comparison was made between patients with stroke and those with tumors and between patients with and without hemiparesis.

Methods

Patients

We retrospectively reviewed MR studies that included diffusion-weighted images from January 1998 to October 1998 and selected those patients with supratentorial tumors and those with supratentorial cerebrovascular disease. We also selected nine control patients who had undergone diffusion-weighted imaging during the same period. The inclusion criteria for the control patients were normal results of their neurologic examinations and MR imaging of the brain. The selected control patients had only minor complaints, such as headache, nausea, and dizziness. Patients with bilateral hemispheric neurologic deficits, involvement of bilateral corticospinal tracts, and infratentorial lesions were excluded from this study. Patients with asymmetrical head positioning and those who moved during diffusion-weighted image acquisition were also eliminated.

Thirty-three patients and nine control patients constituted the study, including 23 men and 19 women (age range, 8–81 years; mean age, 51 years). Eleven patients had tumors (three malignant gliomas, two metastatic tumors, three low-grade gliomas, two brain abscesses, and one unknown nodular tumor), 16 had acute cerebral infarctions less than 2 weeks after ictus (range, 0–14 days; mean, 3.4 days), and four had chronic cerebrovascular disease. Two patients who presented with transient ischemic attacks (hemiparesis) showed no MR abnormality.

Image Acquisition

All MR studies were conducted using a 1.5-T superconducting system. The typical imaging protocol consisted of sagittal T1-weighted (400/14/1 [TR/TE/excitations]) spin-echo, axial T1-weighted (400/14/1) spin-echo, axial T2-weighted (4000–4300/105 [TR/TE_{eff}]; echo train length, 10–12) fast spin-echo, axial and/or coronal fluid-attenuated inversion recovery (10002/148 [TR/effective TE]; inversion time, 2200 ms), and axial diffusion-weighted imaging sequences. For some of the patients, contrast-enhanced T1-weighted (400/14/1) sequences were additionally obtained. For these sequences, with the exception of the diffusion-weighted imaging sequences, the field of view was 20 to 22 cm, the matrix size was 256 × 192, and the section thickness was 5 mm, with a 2.5-mm intersection gap.

Diffusion-weighted images were obtained using multisection single-shot spin-echo echo-planar imaging (10000/98 [TR/

TE_{eff}]). The field of view was 30 × 19 cm, and the matrix size was 128 × 128. The section thickness was 7 mm, with a 3-mm intersection gap, and 11 to 17 axial sections were obtained. The motion-probing gradients were applied sequentially in three orthogonal axes in the direction of the section select (z), phase-encoding (x), and readout (y) gradients, with a b factor of 1000 s/mm², to generate three orthogonal axis diffusion-weighted images (x, y, z). T2-weighted images without motion-probing gradients (b = 0 s/mm²) were also obtained. The patient's head was symmetrically positioned and fixed in the head coil.

Neurologic Findings

We reviewed each patient's medical record for neurologic findings at the time of MR imaging. We paid special attention to motor deficits (hemiparesis), which were graded into four categories: none (no hemiparesis), transient (hemiparesis that disappeared before MR imaging study), slight-mild (hemiparesis but muscles capable of contracting against resistance), and moderate-severe (hemiparesis with muscles incapable of contracting against resistance).

Evaluation of MR Images

Using both conventional MR and diffusion-weighted images, we evaluated the presence or absence of lesional involvement of the supratentorial segments of the corticospinal pathway, including the posterior limb of the internal capsule, the corona radiata, and the cortical or subcortical region around the central sulcus, including sensorimotor cortices.

Data Analysis for Diffusion Anisotropy

The signal intensity (S_i , $i = x, y, z$) on each diffusion-weighted image (x, y, z) is described by $S_i = S_0 \exp(-bD_i)$ ($i = x, y, z$), where S_0 is the signal of the reference image and D_i is the apparent diffusion coefficient in the "i" direction of the motion-probing gradient. We evaluated diffusion anisotropy according to the SD index (A_{SD}) defined by the following formula (27):

$$A_{SD} = \{[(D_x - D_{AV})^2 + (D_y - D_{AV})^2 + (D_z - D_{AV})^2] / 6\}^{1/2} / D_{AV}$$

$$\text{where, } D_{AV} = (D_x + D_y + D_z) / 3.$$

The three-orthogonal diffusion- and T2-weighted images ($b = 0$) were transferred to a workstation for image processing. A_{SD} values were calculated on a pixel-by-pixel basis to generate A_{SD} map images using numerical computation software.

For every case, we selected two or three sections in which the posterior limb of the internal capsule or the corona radiata was included. On each section, the rectangular regions of interest (ROI) were defined in the posterior limb of the internal capsule or the corona radiata on both the affected side and the contralateral unaffected side. To define the ROI on these anatomic structures as accurately as possible, we used our originally developed software. Using this software, three different images of the same section, including the A_{SD} map image, the D_{AV} image, and a selected reference image, were displayed at the same time. When an ROI was defined on the reference image, the location of the ROI was shown on the other two images simultaneously (Fig 1). Because the fiber tracts of the posterior limb of the internal capsule and the corona radiata run in the craniocaudal direction, we used the D_z image as a reference image. These anatomic structures were usually easily identified on the D_z and A_{SD} map images because of their strong anisotropy, and the lesions were identified on the D_{AV} images in most cases. We also referred to the conventional MR images and the three orthogonal diffusion-weighted images for visual comparison.

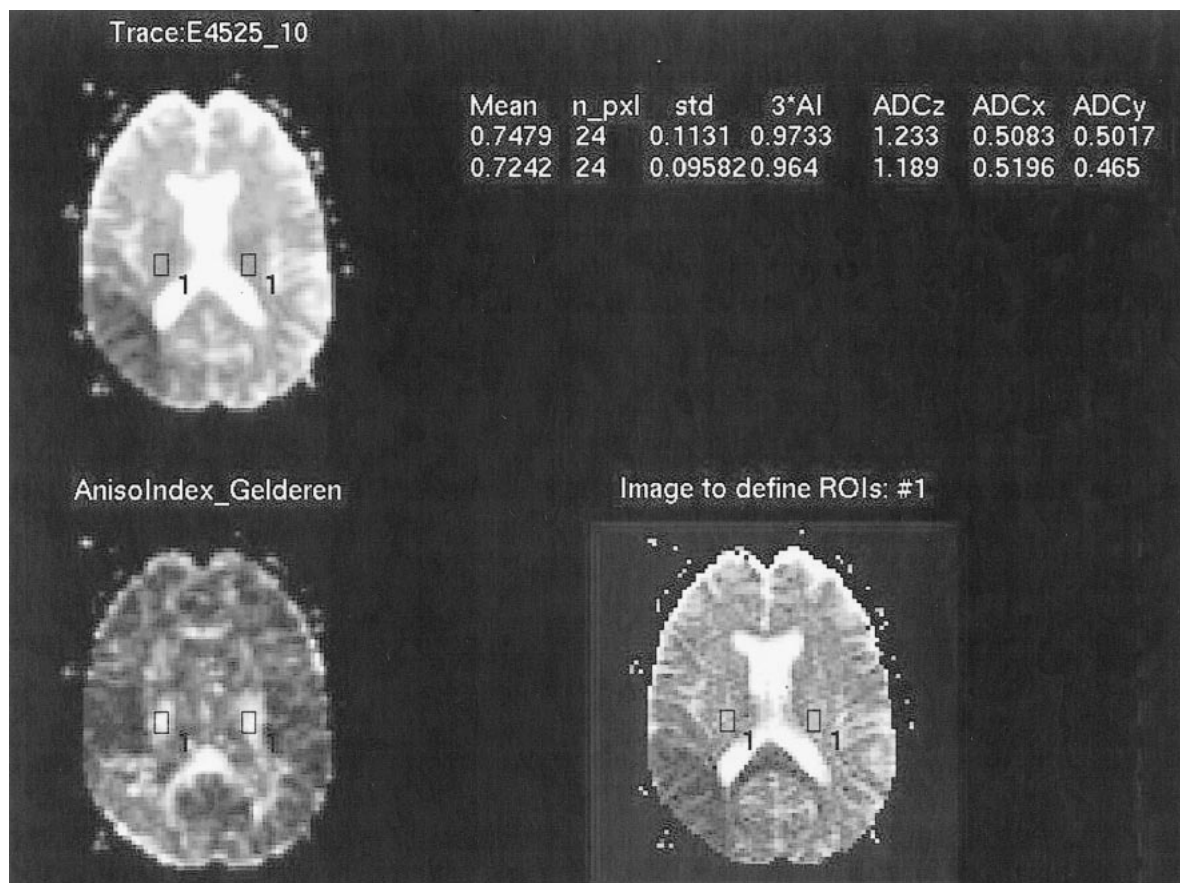


FIG 1. Screen of defining ROI. The D_{AV} image (upper left), the A_{SD} map image (lower left), and the D_z image (lower right) were displayed on the screen, and the location of the defined ROI were shown on the three images simultaneously.

To standardize these ROI values, an asymmetry index (%) of A_{SD} , $AI(A_{SD})$, between the affected side and the contralateral side, was calculated according to the following equation:

$$AI(A_{SD}) = (A_{SD\ cnt} - A_{SD\ aff}) / [(A_{SD\ cnt} + A_{SD\ aff}) / 2] \times 100$$

$A_{SD\ aff}$ and $A_{SD\ cnt}$ represent A_{SD} values from the ROI of the corticospinal tracts on the affected side and the corresponding ROI on the contralateral side, respectively. In cases with hemiparesis, the responsible side for the hemiparesis was regarded as the affected side. In cases with no paresis, the hemisphere having the main lesion was regarded as the affected side. In control cases that had neither hemiparesis nor a lesion, the index was calculated by supposing the left side to be the affected side. The greater the $AI(A_{SD})$ was, the greater was the reduction in anisotropy of the internal capsule or the corona radiata on the affected side. The diffusion anisotropy may change with age. Using the asymmetry index should minimize the influence of age-related change.

These $AI(A_{SD})$ values were compared among the various subgroups classified by the type of lesion that involved the ipsilateral corticospinal tract: control group, uninvolved tract, acute infarction, old cerebrovascular disease, tumor edema, and tumor. We also compared the $AI(A_{SD})$ for various degrees of hemiparesis, including control group, no paresis, transient paresis, slight-mild paresis, and moderate-severe paresis. Statistical analysis was conducted using analysis of variance with Scheffe's post hoc test for multiple comparison. P values less than .05 for multiple comparison were used to determine significant differences.

TABLE 1: Relationship between the degree of hemiparesis and the type of pathologic abnormality

Degree of Hemiparesis	N	MR-revealed Disease			
		No Lesion	Acute Infarct	Old CVD	Tumor
None	11	0	4	3	4
Transient	3	2	1	0	0
Slight-mild	12	0	8	1	3
Moderate-severe	7	0	3	0	4
Total	33	2	16	4	11

Note.—Data in the table represent the number of patients in each category. N: Total number of each category.

Results

According to the medical records, 22 of 33 patients had hemiparesis (Table 1). One patient with transient attacks of hemiparesis had acute infarction in the frontal operculum.

Table 2 shows the relationship between the involved sites of the corticospinal pathway (posterior limb of the internal capsule, the corona radiata, and the sensorimotor cortices) and the degree of hemiparesis. In 21 cases, at least one segment of these structures was involved. Nineteen of these patients

TABLE 2: Relationship between the involved site of the corticospinal pathway and the degree of hemiparesis

Involved Site	N	Degree of Hemiparesis			
		None	Trans- ient	Slight- mild	Mod- erate- severe
No involvement (control)	9	9	0	0	0
No involvement	12	9	3	0	0
Sensory motor cortex (SMC)	3	0	0	3	0
Corona radiata (CR)	8	2	0	3	3
Internal capsule (IC)	2	0	0	2	0
SMC & CR	4	0	0	3	1
IC & CR	4	0	0	1	3
Total	42	20	3	12	7

Note.—Data in the table represent the number of patients in each category. N: Total number of each category for involved site.

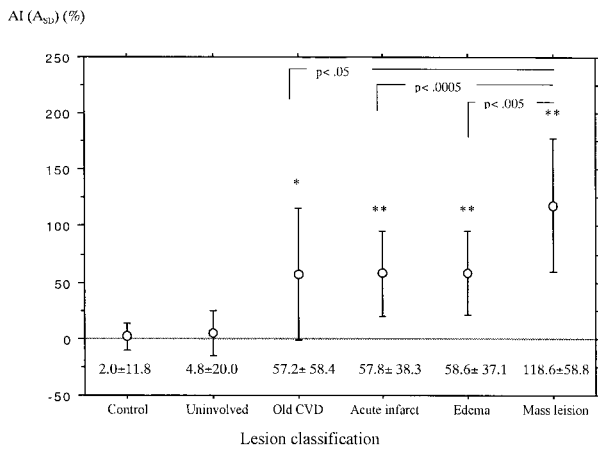


FIG 2. Mean and SD of AI(A_{SD}) of the internal capsule or the corona radiata involved by various types of lesions. Analysis of variance, $F = 39.6$; $P < .0001$; Post hoc test (Scheffe); *, $P = .05$ as compared with the control group; **, $P < .0001$ as compared with both control and uninvolved groups.

showed hemiparesis contralateral to the involved hemisphere. Two patients with involvement of the corona radiata (one with old infarction and the other with a low-grade astrocytoma) showed no hemiparesis.

Figure 2 shows the mean and SD of AI(A_{SD}) of the internal capsule or the corona radiata involved by various lesions. All involved tracts had significantly larger AI(A_{SD}) than did uninvolved and control tracts (Figs 3 and 4). In addition, the mean AI(A_{SD}) of the tracts involved by tumors (mass lesions) was significantly larger than that of tracts involved by the other three lesions.

Figure 5 shows the mean and SD of AI(A_{SD}) for each category, classified by the means of the degree of hemiparesis. The mean AI(A_{SD}) of the cases with moderate-severe hemiparesis was significantly larger than that of the remaining four groups, indicating more decreased diffusion anisotropy of the affected side. The mean AI(A_{SD}) of the group of slight-mild hemiparesis showed a higher value than

that of the control, no paresis, and transient groups, but no significant statistical difference was noted.

As shown in Table 2, at least one segment of the corticospinal pathway from the sensorimotor cortices to the posterior limb of the internal capsule was involved in 21 cases. However, involvement of both the internal capsule and the corona radiata was noted in only four cases. In the remaining 17 cases, either the internal capsule or the corona radiata or both on the affected hemisphere were not involved. We compared the mean AI(A_{SD}) value of the normal-appearing (uninvolved) internal capsule or corona radiata between the 17 patients having some involved segments of the corticospinal tract and the other 21 patients with entirely intact corticospinal tracts (Fig 6). The mean AI(A_{SD}) value of the group having involved segments tended to be larger than that of the group with the intact tract, although a statistically significant difference was not noted. The former group included 12 acute infarctions less than 2 weeks old, four tumors, and one old cerebrovascular disease. Eleven of these patients showed slight-mild hemiparesis, four showed moderate-severe hemiparesis (Fig 3), and two had no paresis. All of them showed no MR finding of Wallerian degeneration.

Discussion

There are six major descending motor control pathways: corticospinal tracts, corticobulbar tracts, vestibulospinal tracts, reticulospinal tracts, rubrospinal tracts, and tectospinal tracts. The former two pathways originate in the cerebral cortex, mainly in the primary motor cortex, and descend through the corona radiata and the posterior limbs of the internal capsule supratentorially. They reach motor nuclei of cranial nerves and other brain stem sites (corticobulbar fibers) or terminate to spinal cord motor neurons and interneurons (corticospinal fibers) (28, 29). Therefore, supratentorial lesions involving the primary motor cortex, corona radiata, or posterior limb of the internal capsule often cause motor deficits. We studied patients with supratentorial lesions and found that 19 (90%) of 21 patients with involvement of these structures had hemiparesis.

The fibers descending through the internal capsule fan out as the corona radiata, just above the internal capsule. The posterior limb of the internal capsule contains not only the corticospinal and corticobulbar fibers but the fibers interconnecting ventroanterior and ventrolateral nuclei of the thalamus with the motor and premotor cortices and some of the somatosensory fibers (28, 29). This means that the involvement of the corona radiata or the posterior limb of the internal capsule does not always produce motor deficits. Two cases, each with a corona radiata lesion, did not show hemiparesis in this series.

In the normal white matter, water molecular motion is unrestricted parallel to the tracts but is hin-

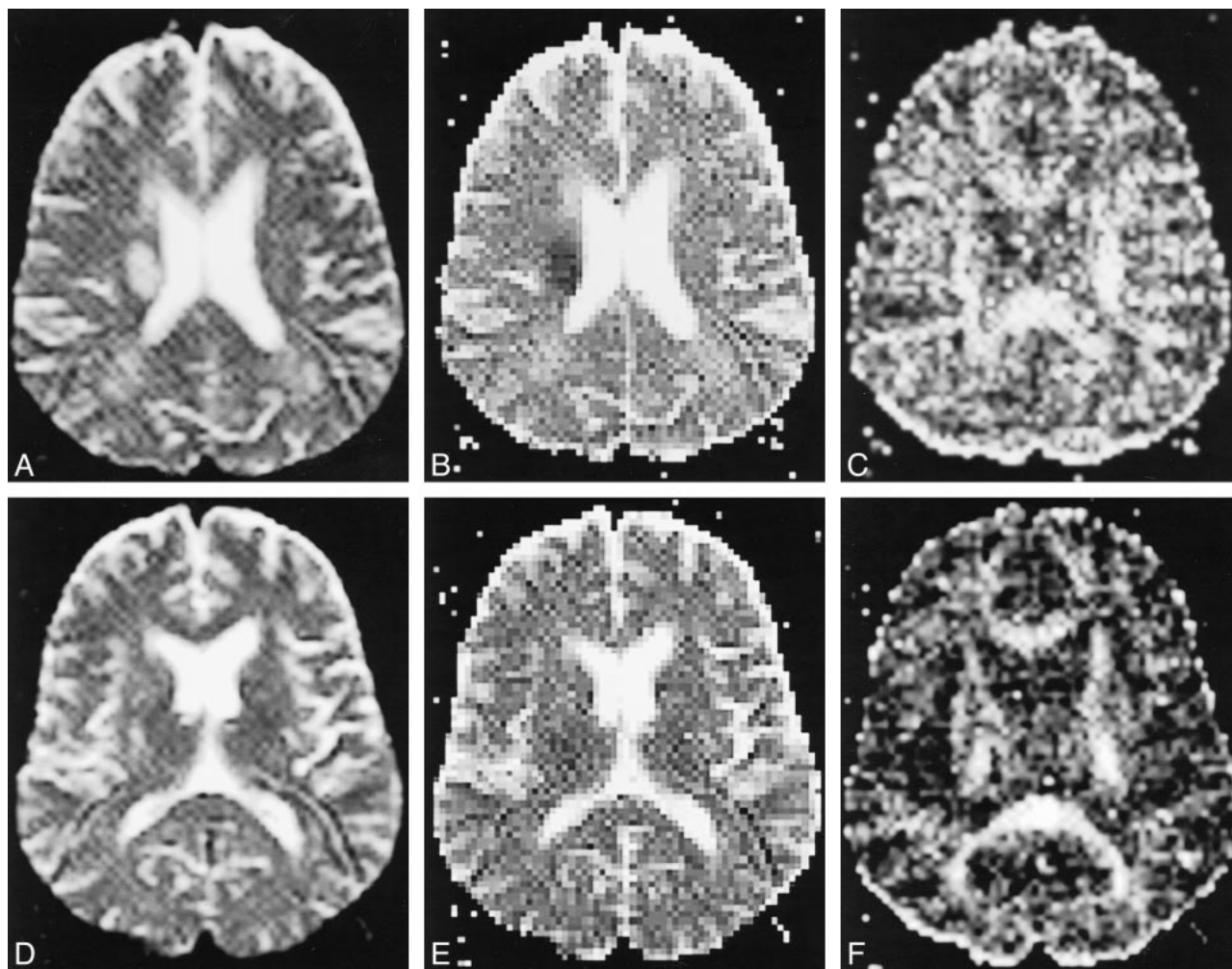


FIG 3. Acute cerebral infarction of the right corona radiata with moderate-severe left hemiparesis.

- A, T2-weighted echo-planar image ($b = 0$) shows an oval hyperintense lesion involving the right corona radiata.
 B, Apparent diffusion coefficient image shows a decreased diffusion coefficient in the lesion.
 C, In the A_{SD} image, the diffusion anisotropy is also reduced.
 D, T2-weighted echo-planar image (10000/98 [TR/TE_{eff}]) that includes the internal capsule shows no involvement of the right internal capsule, although high intensity spotty lesions were noted in the bilateral lentiform nuclei.
 E, Apparent diffusion coefficient image of the same section as that shown in D shows no definite abnormality in the internal capsule.
 F, A_{SD} image shows decreased diffusion anisotropy in the posterior limb of the right internal capsule as compared with the left side.

tered perpendicular to the tracts. This results in directional water diffusion or anisotropy. The diffusion anisotropy may reflect the integrity of the white matter structure. Therefore, impairment of water diffusion in the white matter may correlate with the degree of the damage to its structure. In our measurements, all involved internal capsules and corona radiata showed significantly decreased anisotropy in comparison with uninvolved ones. This reduction of anisotropy means decreased directionality of the water molecular motion in the white matter tracts. This phenomenon may be due to loss of myelin, or replacement of myelinated fibers with glial cells, or abnormal structures such as tumors (24). We found that the diffusion anisotropy was significantly more impaired in the fiber tracts involved by tumors than in those with infarction or peritumoral edema. A possible explanation is that a tumor may be more invasive and may completely

replace the fiber tracts with neoplastic tissue or necrotic tissue in the tumor. In our series, all the tumors that involved the internal capsule or the corona radiata were high-grade gliomas. Our results indicate that the decrease in diffusion anisotropy of the white matter tracts varies for different types of pathologic conditions.

The diffusion anisotropy of the internal capsule or the corona radiata in the affected hemisphere was correlated with the severity of hemiparesis. Inoue et al (18) evaluated the continuity of the pyramidal tract in patients with brain tumors near the tract by using 3D anisotropy contrast MR images, which were composed by combining color-coded diffusion-weighted images with three orthogonal motion-probing gradients to delineate the fiber trajectory (19). On the 3D anisotropy contrast images, they could easily differentiate discontinuity of the tract due to impaired anisotropy from compression

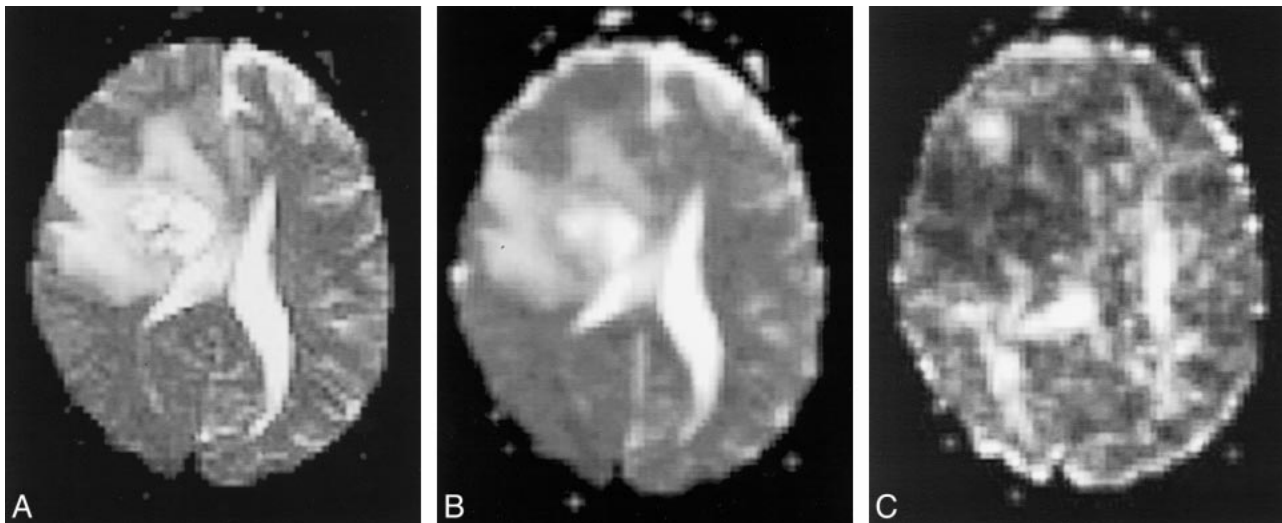


FIG 4. Glioblastoma involving the right corona radiata and basal ganglia with moderate-severe hemiparesis. A, T2-weighted echo-planar image shows an irregular mass with marked perifocal edema involving the right corona radiata. B, Apparent diffusion coefficient image shows an irregular mass with marked perifocal edema involving the right corona radiata. C, In the A_{SD} image, the diffusion anisotropy of the right corona radiata is hardly noted.

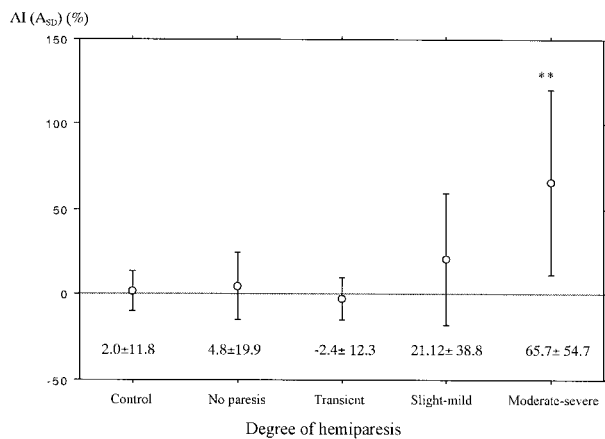


FIG 5. Mean and SD of $AI(A_{SD})$ of the internal capsule or the corona radiata for each degree of hemiparesis. Analysis of variance, $F = 17.0$; $P < .0001$; Post hoc test (Bonferroni); *, $P < .0001$ as compared with every other group.

of the tract by the mass effect and showed good correlation between the findings and the pre- and postoperative motor functions. Karibe et al (20) studied patients with deep intracerebral hemorrhage by use of anisotropic diffusion-weighted imaging and evaluated the correlation between motor function and corticospinal tract injury on diffusion-weighted images obtained at admission. Initial corticospinal tract injury was not correlated with the motor impairment at admission but was closely correlated with motor impairment 1 month after onset. They concluded that early evaluation of corticospinal tract injury using diffusion-weighted imaging could provide predictive value for motor function outcome in patients with cerebral hemorrhage. In these two studies, the continuity of the fiber tracts on diffusion-weighted images was visually evaluated. In a quantitative evaluation,

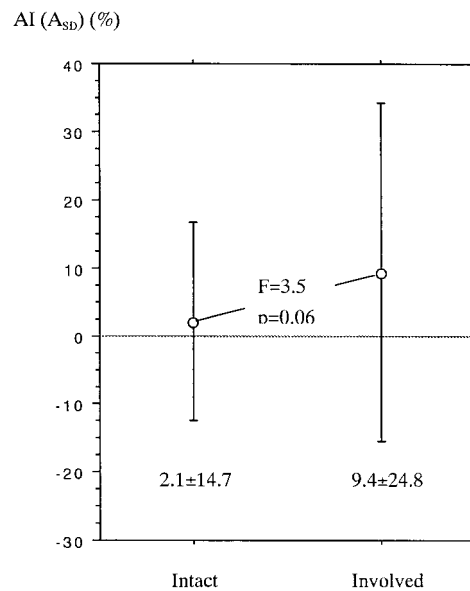


FIG 6. Comparison of $AI(A_{SD})$ value (mean and SD) of normal-appearing internal capsule and corona radiata between the patients with entirely intact corticospinal tract (*Intact*) and those having some involved segments of the corticospinal tract (*Involved*).

Wieshmann et al (24) measured the diffusion tensor in the coronae radiata in patients with chronic hemiparesis caused by supratentorial lesions. In all cases, the anisotropy was reduced in the coronae radiata contralateral to the hemiparesis by more than 3 SD compared with control participants, although the significant difference was not noted between patients with mild hemiparesis and those with severe hemiparesis. In our results, however, the diffusion anisotropy of the moderate-severe hemiparesis group was significantly reduced as compared with other groups. The study by Wieshmann et al included only cases with chronic hemi-

paralysis, whereas we studied different types of pathologic conditions, including tumors and acute and chronic infarctions. These different constituents may have affected the differing results.

In the cases having some segments of the corticospinal tract involved by pathologic abnormality, the diffusion anisotropy tended to be reduced not only in the involved segments but also in the apparently uninvolved segments on the affected side. Several investigators have reported similar findings. Pierpaoli et al (25) reported decreased anisotropy in the midbrain and medulla oblongata of the affected side by measuring the diffusion tensor in patients with chronic supratentorial infarction. Wieshmann et al (24) showed the reduction of anisotropy in the cerebral peduncle remote from supratentorial lesions in patients with severe chronic hemiparesis. A possible explanation for such phenomena is wallerian degeneration of the fiber tracts secondary to the supratentorial lesion. The wallerian degeneration along the corticospinal tracts is usually detected at 4 weeks after cerebral infarction as a hypointense signal band on conventional T2-weighted images. It then becomes hyperintense after 10 to 14 weeks and finally results in hemiatrophy of the brain stem (30). These two reports of reduced anisotropy dealt with patients with chronic disease. Our cases included patients with acute infarction of less than 2 weeks' duration and no detectable wallerian degeneration on standard MR images. This shows that evaluation of the anisotropy might detect wallerian degeneration or some secondary degenerative change in white matter earlier and with greater sensitivity than conventional MR imaging.

There have been some reports regarding the relationship between wallerian degeneration and clinical findings. Wallerian degeneration of the pyramidal tracts was often found in patients with capsular infarction, especially when associated with motor deficit (31). Orita et al (32) measured an area of wallerian degeneration in the pons on T2-weighted coronal images in patients with cerebrovascular disease of the internal capsule and concluded that the area of wallerian degeneration was related to the severity of the motor deficit. Watanabe and Tashiro (33) and Sawlani et al (34) compared the functional prognosis between patients with and without wallerian degeneration and found that the presence of wallerian degeneration correlated well with persistent functional disability. Therefore, the measurement of the diffusion anisotropy might help to predict the functional prognosis of patients earlier in the acute stage of infarction. Igarashi et al (17) evaluated the change in diffusion anisotropy associated with wallerian degeneration of the pyramidal tracts in patients with supratentorial cerebrovascular accidents by use of 3D anisotropy contrast MR images. Patients examined during the acute stage who later recovered from hemiparesis had no visible changes on the 3D anisotropy contrast images, whereas patients who

recovered poorly showed distinct color fading in the pyramidal tract within 14 days after stroke.

Our study had several limitations. We did not have software to obtain diffusion tensor imaging on our MR imaging unit, so we could not measure the diffusion tensor exactly. The study was limited to evaluate the diffusion anisotropy by using data with three orthogonal diffusion gradients. Because most of the white matter fibers pass obliquely to the magnet coordinates, the diffusion anisotropy calculated by three-directional diffusion-weighted imaging tends to be underestimated and the measured values are also rotationally variant (15, 16). The more accurate measurement of the diffusion anisotropy exactly along each fiber orientation requires diffusion tensor imaging, with at least nine different directional motion-probing gradients. To minimize errors associated with our incomplete measurements, we standardized the value using an asymmetry index. However, such incomplete measurements of the diffusion anisotropy can lead to erroneous results, especially in some patients with brain tumors in which the white matter fibers are distorted asymmetrically because of the mass effect. This measurement error intrinsic to this study might partly account for the markedly impaired anisotropy in the tracts involved by tumors as compared with that in tracts involved by other lesions. More exact evaluation by diffusion tensor measurement is required for further clarification. The number of cases in our study was too small to analyze statistically the reduction of the diffusion anisotropy between various types of pathologic conditions involving the tracts and the degree of motor impairment separately. Another limitation of our study was that the control group consisted of patients, not of healthy volunteers. However, we carefully selected patients who did not have any neurologic signs and who had normal results of MR imaging of the brain as the control patients. Despite these limitations, our results show some consistency with those of previous reports (24, 25, 32).

Conclusion

The diffusion anisotropy in the posterior limb of the internal capsule or the corona radiata was significantly reduced in cases with involvement to these structures by infarction or tumor. This decrease in anisotropy was more prominent in the tracts involved by tumors than in those involved by infarction/edema and was correlated with the severity of hemiparesis. The diffusion anisotropy tended to be also impaired in normal-appearing fiber tracts remote from the involved segment of the corticospinal tract. Although more exact measurements of the diffusion tensor are required, we think that evaluating diffusion anisotropy may provide additional information relating to neurologic function and transneuronal effects.

References

- Taylor DG, Bushell MC. **The spatial mapping of translational diffusion coefficients by the NMR imaging technique.** *Phys Med Biol* 1985;30:345-349
- Le Bihan D, Breton E, Lallemand D, Grenier P, Cabanis E, Laval-Jeantet M. **MR imaging of intravoxel incoherent motions: application to diffusion and perfusion in neurologic disorders.** *Radiology* 1986;161:401-407
- Krabbe K, Gideon P, Wagn P, Hansen U, Thomsen C, Madsen F. **MR diffusion imaging of human intracranial tumors.** *Neuroradiology* 1997;39:483-489
- Beauchamp Jr NJ, Ulug AM, Passe TJ, van Zijl PCM. **MR diffusion imaging in stroke: review and controversies.** *Radiographics* 1998;18:1269-1283
- Brunberg JA, Chenevert TL, McKeever PE, et al. **In vivo MR determination of water diffusion coefficients and diffusion anisotropy: correlation with structural alteration in gliomas of the cerebral hemispheres.** *AJNR Am J Neuroradiol* 1995;16(2):361-371
- Provenzale JM, Sorensen AG. **Diffusion-weighted MR imaging in acute stroke: theoretic considerations and clinical applications.** *AJR Am J Roentgenol* 1999;173(6):1459-1467
- Christiansen P, Gideon P, Thomsen C, Stubgaard M, Henriksen O, Larsson HBW. **Increased water self-diffusion in chronic plaques and in apparently normal white matter in patients with multiple sclerosis.** *Acta Neurol Scand* 1993;87:195-199
- Droogan AG, Clark CA, Werring DJ, Barker GJ, McDonald WI, Miller DH. **Comparison of multiple sclerosis clinical subgroups using navigated spin echo diffusion-weighted imaging.** *Magn Reson Imaging* 1999;17(5):653-661
- Larsson HBW, Thompsen C, Frederiksen J, Stubgaard M, Henriksen O. **In vivo magnetic resonance diffusion measurement in the brain of the patients with multiple sclerosis.** *Magn Reson Imaging* 1992;10:7-12
- Tievsky AL, Ptak T, Farkas J. **Investigation of apparent diffusion coefficient and diffusion tensor anisotropy in acute and chronic multiple sclerosis lesions.** *AJNR Am J Neuroradiol* 1999;20(8):1491-1499
- Chenevert TL, Brunberg JA, Pipe JG. **Anisotropic diffusion in human white matter: demonstration with MR techniques in vivo.** *Radiology* 1990;177(2):401-405
- Le Bihan D, Turner R, Douek P. **Is water diffusion restricted in human brain white matter? An echo-planar NMR imaging study.** *Neuroreport* 1993;4(7):887-890
- Moseley ME, Kucharczyk J, Asgari HS, Norman D. **Anisotropy in diffusion-weighted MRI.** *Magn Reson Med* 1991;19(2):321-326
- Sakuma H, Nomura Y, Takeda K, et al. **Adult and neonatal human brain: diffusional anisotropy and myelination with diffusion-weighted MR imaging.** *Radiology* 1991;180(1):229-233
- Pierpaoli C, Basser PJ. **Toward a quantitative assessment of diffusion anisotropy.** *Magn Reson Med* 1996;36(6):893-906
- Pierpaoli C, Jezzard P, Basser PJ, Barnett A, Di Chiro G. **Diffusion tensor MR imaging of the human brain.** *Radiology* 1996;201(3):637-648
- Igarashi H, Katayama Y, Tsuganezawa T, Yamamuro M, Terashi A, Owan C. **Three-dimensional anisotropy contrast (3DAC) magnetic resonance imaging of the human brain: application to assess wallerian degeneration.** *Intern Med* 1998;37(8):662-668
- Inoue T, Shimizu H, Yoshimoto T. **Imaging the pyramidal tract in patients with brain tumors.** *Clin Neurol Neurosurg* 1999;101(1):4-10
- Nakada T, Matsuzawa H. **Three-dimensional anisotropy contrast magnetic resonance imaging of the rat nervous system: MR axonography.** *Neurosci Res* 1995;22(4):389-398
- Karibe H, Shimizu H, Tominaga T, Kosu K, Yoshimoto T. **Diffusion-weighted magnetic resonance imaging in the early evaluation of corticospinal tract injury to predict functional motor outcome in patients with deep intracerebral hemorrhage.** *J Neurosurg* 2000;92(1):58-63
- Nakada T, Nakayama N, Fujii Y, Kwee IL. **Clinical application of three-dimensional anisotropy contrast magnetic resonance axonography.** *J Neurosurg* 1999;90(4):791-795
- Yang Q, Tress BM, Barber PA, et al. **Serial study of apparent diffusion coefficient and anisotropy in patients with acute stroke.** *Stroke* 1999;30(11):2382-2390
- Sorensen AG, Wu O, Copen WA, et al. **Human acute cerebral ischemia: detection of changes in water diffusion anisotropy by using MR imaging.** *Radiology* 1999;212(3):785-792
- Wieshmann UC, Clark CA, Symms MR, Franconi F, Barker GJ, Shorvon SD. **Anisotropy of water diffusion in corona radiata and cerebral peduncle in patients with hemiparesis.** *Neuroimage* 1999;10(2):225-230
- Pierpaoli C, Barnett A, Virda A, Penix L, Chen R. **Diffusion MRI of wallerian degeneration: a new tool to investigate neural connectivity in vivo?** Presented at the 6th Scientific Meeting of the ISMRM, Sydney, 1998
- Jones DK, Lythgoe D, Horsfield MA, Simmons A, Williams SC, Markus HS. **Characterization of white matter damage in ischemic leukoaraiosis with diffusion tensor MRI.** *Stroke* 1999;30(2):393-397
- van Gelderen P, de Vleeschouwer MH, DesPres D, Pekar J, van Zijl PC, Moonen CT. **Water diffusion and acute stroke.** *Magn Reson Med* 1994;31(2):154-163
- Martin JH. *Neuroanatomy: Text and Atlas.* Amsterdam: Elsevier Science Publishing; 1989
- Nolte J. *The Human Brain: An Introduction to Its Functional Anatomy.* 4th ed. St. Louis: Mosby-Year Book; 1999
- Kuhn MJ, Mikulis DJ, Ayoub DM, Kosofsky BE, Davis KR, Taveras JM. **Wallerian degeneration after cerebral infarction: evaluation with sequential MR imaging.** *Radiology* 1989;172(1):179-182
- Pujol J, Marti-Vilalta JL, Junque C, Vendrell P, Fernandez J, Capdevila A. **Wallerian degeneration of the pyramidal tract in capsular infarction studied by magnetic resonance imaging.** *Stroke* 1990;21(3):404-409
- Orita T, Tsurutani T, Izumihara A, Kajiwara K, Matsunaga T. **Pyramidal tract wallerian degeneration and correlated symptoms in stroke.** *Eur J Radiol* 1994;18(1):26-29
- Watanabe H, Tashiro K. **Brunnstrom stages and wallerian degenerations: a study using MRI.** *Tohoku J Exp Med* 1992;166(4):471-473
- Sawlani V, Gupta RK, Singh MK, Kohli A. **MRI demonstration of wallerian degeneration in various intracranial lesions and its clinical implications.** *J Neurol Sci* 1997;146(2):103-108